PHYSICAL REVIEW B VOLUME 18, NUMBER 7 1 OCTOBER 1978

Resonant coupling of shear waves in magnetostrictive rare-earth–iron compounds

Stefano Rinaldi*
Naval Surface Weapons Center, Silver Spring, Maryland 20910
and American University, Washington, DC 20016

James Cullen†
Naval Surface Weapons Center, Silver Spring, Maryland 20910
(Received 13 March 1978)

The possibility of altering the direction of polarization of [110] shear waves in cubic ferromagnets is discussed. Using conventional magnetoelastic theory and known elastic and magnetoelastic parameters it is predicted that in $Tb_{0.3}Dy_{0.7}Fe_2$ it is possible, by rotating an applied magnetic field in the (110) plane, to change the polarization of an incident wave by 90°. The acoustical amplitude in a receiving transducer whose axis was perpendicular to that of the transmitting one was measured in fields from 4 to 10 kOe. The amplitude as a function of orientation is sharply peaked at the angle of field at which a rapid change in normal-mode polarization is predicted.

I. INTRODUCTION

The elastic properties of solids are completely determined once their elastic constants are given. In particular, three such constants are sufficient to determine the elastic properties of cubic solids.[1] In magnetically ordered solids which are otherwise cubic the overall symmetry is lowered and depends on the moment direction. Thus, in principle, additional elastic constants are required for a sufficient description of the elasticity. The principal effect of the additional elastic constants is to change the character of the normal modes of vibration.

For example, symmetry breaking in a magnetic field has been observed in Ni using shear waves propagating in the [001] direction,[2] while a saturating magnetic field was applied in the (001) plane. The (001) plane is elastically isotropic; the presence of a magnetic moment provides a unique axis of polarization. Waves polarized parallel to it travel more slowly than those perpendicular to it. These are the appropriate polarizations of the normal modes in this case. There should also be an effect on the polarization in elastically anisotropic planes [e.g., (110)] where there is a competition between the crystal axes and the moment direction for control of the ultimate polarization axes. However, even in magnetostrictive crystals, the effects of magnetoelastic coupling on the elastic tensor are so small that changes in character of acoustical waves (e.g., polarization rotation) in these planes are not amenable to study. Measurements instead have been made of changes in the three cubic constants, C_{11}, C_{12}, and C_{44}. These changes are of the order of 10^{-3} in magnetically saturated Ni,[3] 10^{-4} in YIG.[4] There are, however, exceptional cases of cubic systems, namely, rare-earth compounds with iron, which are ordered magnetically and have very large magnetoelastic coupling. For example, the magnetostriction[5] in $TbFe_2$ is nearly 10^{-3} even at room temperature. Recent ultrasonic experiments[6] confirm the large coupling and show that relative changes in C_{44} of 50% in the pseudobinary $Tb_{0.3}Dy_{0.7}Fe_2$ could be achieved even with the sample magnetically saturated. It is our purpose here to explore the competition between elastic anisotropy and magnetoelastic coupling in this material by looking at the change in polarization of shear waves propagating in the [110] direction. The experiment consisted in measuring the acoustical output at a receiving transducer arranged with its axis perpendicular to that of a sending one at the opposite end of a single-crystal [110] rod. For a review of the magnetoelastic properties of rare-earth iron alloys, see Ref. 10.

The (110) plane is elastically anisotropic. Any wave initially polarized along an arbitrary direction in this plane is broken up into two linearly polarized normal modes, one along [001] and one along $[\bar{1}10]$ in a nonmagnetic crystal. Because of this elastic anisotropy, the presence of a moment in the (110) plane and a finite magnetoelastic coupling will not completely tilt the axis of polarization from, say, [001] to parallel to the moment. The tilt angle Φ will instead lie between these two directions (see Fig. 1). Φ is determined by the ratio of the appropriate off-diagonal elastic constant B to the difference in cubic shear moduli, $C_{44}-\frac{1}{2}(C_{11}-C_{12})$. Now B, according to the linear theory of magnetoelasticity, is of the order of the modification in C_{44} or $C_{11}-C_{12}$ themselves, i.e., $10^{-3}C_{44}$ in Ni but $0.5C_{44}$ in $Tb_{0.3}Dy_{0.7}Fe_2$. Since $C_{44}-\frac{1}{2}(C_{11}-C_{12})$ is about $0.25C_{44}$ in $Tb_{0.3}Dy_{0.7}Fe_2$, we expect a significant tilting of the polarization

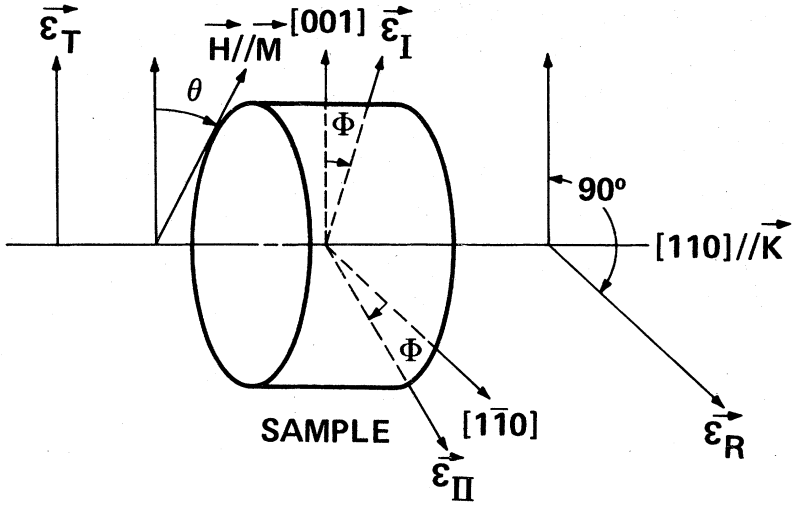

FIG. 1. Schematic view of the experimental arrangement. $\vec{\epsilon}_T$ and $\vec{\epsilon}_R$ are the polarizations of the transmitting and receiving transducers, respectively. Also depicted are a typical magnetic field orientation θ and normal mode polarizations Φ, both in the (110) plane.

in the latter. Further, C_{44} is lowered by the magnetoelastic coupling, lowered from a value greater than to a value less than $\frac{1}{2}(C_{11}-C_{12})$ (which is only modified by a percent) by rotating the moment from [$\bar{1}$10] to [001]. Under this operation, Φ is rotated by 90°. Since most of the change in Φ should come when the magnetization is oriented to make the cubic moduli equal, there should be a sudden appearance of amplitude at the receiver as a magnetic field is rotated into the vicinity of this special orientation.

Formulas for the tilt and velocity of both normal modes are derived in Sec. II, where in addition the amplitude at the receiving transducer is predicted as a function of the angle the moment makes with the [001] direction in the (110) plane. The theoretical amplitude is a product of a smooth function with a maximum at the angle for which the modified C_{44} modulus equals $\frac{1}{2}(C_{11}-C_{12})$ and an oscillating function due to interferences between the amplitudes of the two normal modes.

The experiment is described and the results discussed in Sec. III. The experimental amplitude was measured as a function of orientation of a magnetic field applied in the (110) plane and was in rather good agreement with the predictions. In Sec. IV we discuss the relative contributions first- and second-order elastic constants may be making to the tilting of the polarization. Finally, we point out the utility of making transmission measurements as a function of the magnitude of an applied field fixed in orientation.

II. VELOCITIES AND POLARIZATIONS

Our aim here is to develop the appropriate formulas for the change in velocity and polarization of the normal modes as a function of magnetic field orientation. We begin with the well-known expression for the magnetoelastic energy density involving the components of the magnetization M_i and strain ϵ_{ij}.[7] Including only terms quadratic in the magnetization and linear in the strain, for cubic materials we have

$$E_{\text{me}}=\frac{b_1}{M_s^2}\sum_i\left(M_i^2-\frac{1}{3}\right)\epsilon_{ii}+\frac{b_2}{M_s^2}\sum_{i\neq j}\epsilon_{ij}M_iM_j\,, \tag{1}$$

where M_s is the saturation magnetization. Here b_1 and b_2 are the usual magnetoelastic coupling constants. We have defined the strain as

$$\epsilon_{ij}=\frac{1}{2}\left(\frac{\partial u_i}{\partial x_j}+\frac{\partial u_j}{\partial x_i}\right)\,, \tag{2}$$

where the u_i are the displacement components and x_i the components of the position vector. Letting E to be the total energy density, i.e., the sum of the magnetic, elastic,[1] and magnetoelastic energy densities, the equations of motion for the M_i and the u_i are written [for waves varying in time as $\exp(-i\omega t)$]

$$-\rho\omega^2u_i=\frac{\partial}{\partial x_i}\frac{\partial E}{\partial E_{ij}} \tag{3}$$

and

$$\frac{\partial\vec{\mathrm{M}}}{\partial t}=\gamma\left(\vec{\mathrm{M}}\times\frac{\partial E}{\partial\vec{\mathrm{M}}}\right)\,, \tag{4}$$

where ρ is the density and γ is the gyromagnetic ratio.

In what follows we assume the applied magnetic field H_0 to be in the (110) plane and large enough to saturate the crystal magnetically. At frequencies in the ultrasonic range we can set the left-hand side of Eq. (4) equal to zero. We are interested in plane-wave solutions propagating as $\exp(-i\vec{q}\cdot\vec{x})$ where $\vec{q}$ is parallel to the [110] direction. Taking a coordinate system with the z axis

parallel to [001], x parallel to [100], and y parallel to [010], the equations of motion for the transverse displacements u_z and $u_x - u_y$ ($\equiv u_t$) become

$$\rho\omega^2 u_t = q^2 u_t\left(\frac{C_{11}-C_{12}}{2} - \frac{b_1 M_x^2}{M_s^3 H}\right) - q^2 u_z b_1 b_2 \frac{M_x M_z}{M_s^3 H} , \tag{5}$$

$$\rho\omega^2 u_z = q^2 u_z\left(C_{44} - \frac{b_2^2 M_z^3}{M_s^3 H}\right) - q^2 u_t b_1 b_2 \frac{M_x M_z}{M_s^3 H} . \tag{6}$$

In these equations, H is the magnitude of the total field, the sum of the applied field and an internal field, $4\pi\vec{M}_s + H_a$. The $4\pi M_s$ contribution[8] takes into account the fact that we are working at wavelengths much smaller than the skin depth. The orientation-dependent contribution H_a comes from magnetocrystalline anisotropy.[9] Note that a combination of constants $b_1 b_2$ couples [001] and [$\bar{1}$10] vibrations for general orientations of $\vec{M}$. The polarizations of the normal modes remain 90° apart but are tilted away from these crystalline axes. If we let θ and Φ be, respectively, the angle the moment and one of the polarizations make with the [001] axis so that

$$u_t = \sin\Phi, \quad u_z = \cos\Phi , \tag{7}$$

and

$$M_x/M_s = \sin\theta , \quad M_z/M_s = \cos\theta , \tag{8}$$

then Eqs. (5) and (6) become

$$\rho\frac{\omega^2}{q^2}\sin\Phi = \left(\frac{C_{11}-C_{12}}{2} - \frac{b_1^2\sin^2\theta}{M_s H}\right)\sin\Phi - b_1 b_2 \frac{\sin 2\theta}{2M_s H}\cos\Phi , \tag{9}$$

$$\rho\frac{\omega^2}{q^2}\cos\Phi = \left(C_{44} - \frac{b_2^2\cos^2\theta}{M_s H}\right)\cos\Phi - b_1 b_2 \frac{\sin 2\theta}{2M_s H}\sin\Phi . \tag{10}$$

Solving the secular equation for $(\omega/q)^2$ gives the normal-mode velocities:

$$\rho v_\pm^2 = \tfrac{1}{2}(C'+C) \pm \{[\tfrac{1}{2}(C'-C)]^2 + B^2\}^{1/2} , \tag{11}$$

where

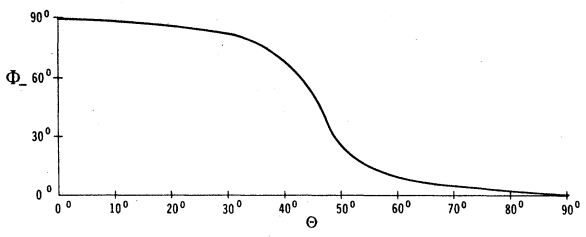

FIG. 2. Behavior of the polarization angle Φ_- with magnetic field orientation θ for $Th_{0.3}Dy_{0.7}Fe_2$ based on Table I and Eq. (13) of the text. Note that sharp drop in Φ_- predicted for the orientation for which the velocities of the normal modes come closest to being equal (Fig. 3). The external field was set equal to 8 kOe for this calculation.

$$\begin{aligned} C &\equiv C_{44} - b_2^2\cos^2\theta/M_s H , \\ C' &\equiv (C_{11}-C_{12})/2 - b_1^2\sin^2\theta/M_s H , \\ B &\equiv b_1 b_2 \frac{\sin 2\theta}{2HM_s} . \end{aligned} \tag{12}$$

Using these definitions and Eq. (11), the expression for the polarization tilt can be written

$$\tan\Phi_\pm = -B\{\tfrac{1}{2}(C-C') \pm [\tfrac{1}{2}(C'-C)^2 + B^2]^{1/2}\}^{-1} . \tag{13}$$

Φ_+ and Φ_- refer to the tilt from the [001] of the two normal modes.

From Eq. (13) it is clear that Φ_+ is small (and Φ_- near 90°) if $B/|C-C'|$ is small, which is the situation usually encountered. As we pointed out in Sec. I, velocity measurements in $Tb_{0.3}Dy_{0.7}Fe_2$ have shown that $C < C'$ for $\theta = 0°$, whereas $C > C'$ for $\theta = 90°$; at some θ therefore C' must be equal to C. Φ_- is not 90° but changes from 90° to 0°, passing 45° at $C = C'$. Thus, for this material it should be possible to rotate the polarization of a wave initially along the [001] direction sufficiently so that the polarization is finally along [$\bar{1}$10]. Figure 2 shows Φ_- plotted as a function of θ using the measured[6] parameters of $Tb_{0.3}Dy_{0.7}Fe_2$ listed in Table I, taking $b_1 = 0.1 b_2$, H_a independent of θ and equal to 10 kOe. Note the sharp drop in Φ_- from

TABLE I. Parameters used in the calculations of velocity and polarization for $Tb_{0.3}Dy_{0.7}Fe_2$. The elastic and magnetoelastic constants are in Dyn/cm^2.

C_{44}	C_{11}-C_{12}	$\lvert b_2\rvert$	$\lvert b_1\rvert$	M_s (kOe)	ρ (g/cm^3)
4.86×10^{11}	7.62×10^{11}	2.3×10^{9}	2.3×10^{8}	800	9.21

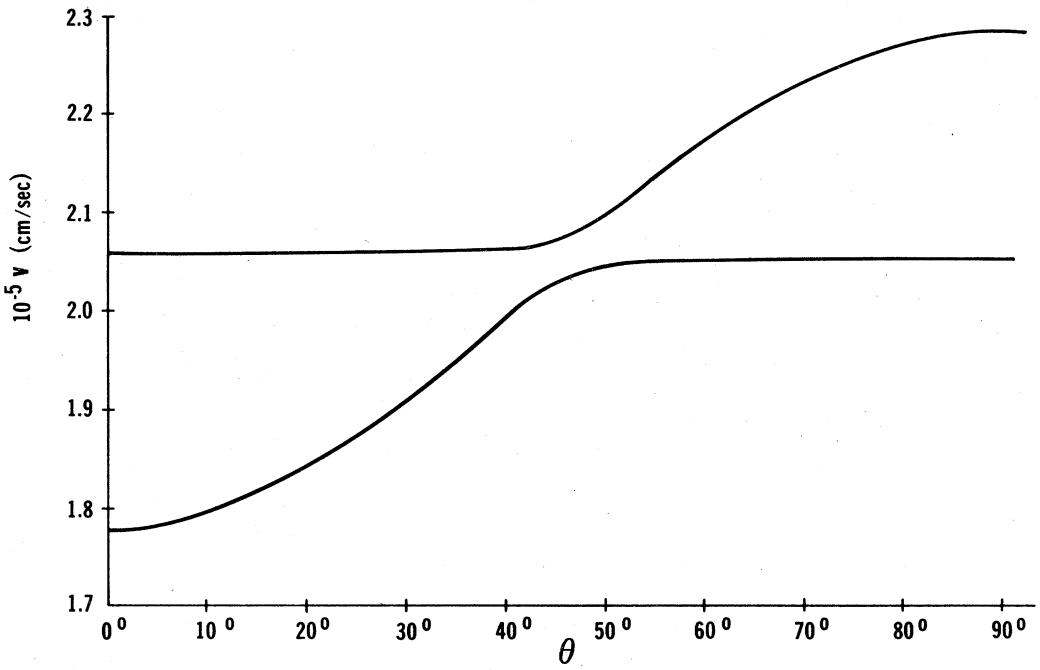

FIG. 3. Velocities of the two shear modes as a function of magnetic field orientation, calculated using Eqs. (11) and (12) and Table I. The external field is 8 kOe. If b_1 were zero, the two curves would have intersected near $\theta = 45°$.

90° to almost zero for θ around 40°. In Fig. 3, we have plotted the velocities of both normal modes using the same set of parameters. The velocities are never equal; they are nearly so only in that region of θ where Φ is changing rapidly, i.e., where $C \approx C'$.

Similar resonancelike effects are expected for a fixed θ as the magnitude of the external field

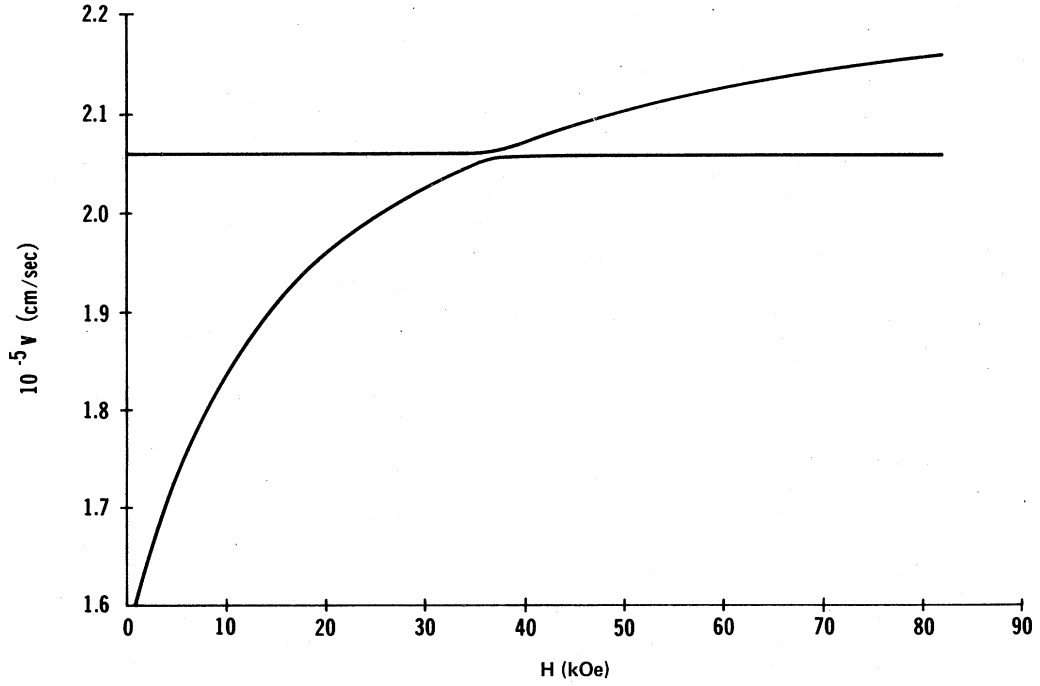

FIG. 4. Velocities of the two shear modes as a function of magnetic field strength, calculated using Eqs. (11) and Eqs. (12) and Table I, and setting the field orientation at 10° from the [001] axis.

is changed. A plot, again using $Tb_{0.3}Dy_{0.7}Fe_2$ parameters, is given of the velocities versus H in Fig. 4. The applied field in this plot is 10° from the [001] direction, in the (110) plane. Unfortunately the predicted resonance field of 43 kOe is beyond the capacity of our magnet.

III. TRANSMISSION EXPERIMENT

To measure the rotation of the axes of polarization of the normal modes we performed a room-temperature transmission experiment whose arrangement is schematically shown in Fig. 1. A shear wave with polarization ϵ_T parallel to the [001] axis was generated by a transmitting transducer bonded using a highly viscous liquid (Parametrics Shear Couplant) on a (110) face of a 3-mm-thick single-crystal sample of $Tb_{0.3}Dy_{0.7}Fe_2$. A receiving transducer was mounted on the opposite (110) face but with polarization $\vec{\epsilon}_R$ parallel to the $[1\bar{1}0]$ axis and hence perpendicular to $\vec{\epsilon}_T$. The resonant frequency of both transducers was 12 MHz. The sample holder was supported between the pole faces of an electromagnet in such a way that a field up to 10 kOe could be applied in (110) plane at any angle from the [001] axis. It is clear that when the normal modes are parallel to the crystallographic axis no signal can be detected by the receiver. When the normal modes are tilted by an angle $\Phi \neq 0$ the incoming wave partially excites both normal modes which then propagate independently. It is easy to show that under these conditions the amplitude of the signal detected by the receiver is

$$R = \sin 2\Phi \sin[\omega L(v_+ - v_-)/2v_+v_-], \qquad (14)$$

where ω is the frequency, L is the thickness of the sample, and the attenuation has been assumed equal for both the normal modes. This latter assumption is in keeping with our experience from pulse-echo experiments, in which we observe very little difference in attenuation of $C_{11} - C_{12}$ and C_{44} modes above 4 kOe. Further, the attenuation was small above this field, with no noticable change as the angle of the magnetic field varied in the (110) plane. (There was significant attenuation even at 8 kOe when the field had a large component out of this plane.) The first term of the right-hand side of Eq. (14) accounts for the projection of the incoming shear waves onto the normal-mode axes and then back to the receiver axis; the second term is due to the interference between the components of the normal modes paralel to the receiver axis.

Equation (14) is the result of a continuous-wave analysis of the experiment, whereas 1-μsec pulses were actually employed. These pulses were longer than the separation in time between the two normal-mode signals, yet shorter than the time required for the combined signal to pass through the system of transducers, two delay rods, and the sample. Generalizing the analysis slightly by forming a Gaussian packet of waves like that of Eq. (14), we calculated an amplitude equal to Eq. (14) evaluated at the carrier frequency times an exponential factor that depended only weakly on angle. We thus expect Eq. (14) to be a good representation of the angular dependence of the amplitude of the combined signal. (The transducers used in this experiment were 41°-rotated X-cut $LiNbO_3$ crystals.)

Using the same set of parameters listed above for $Tb_{0.3}Dy_{0.7}Fe_2$ we have calculated the expected

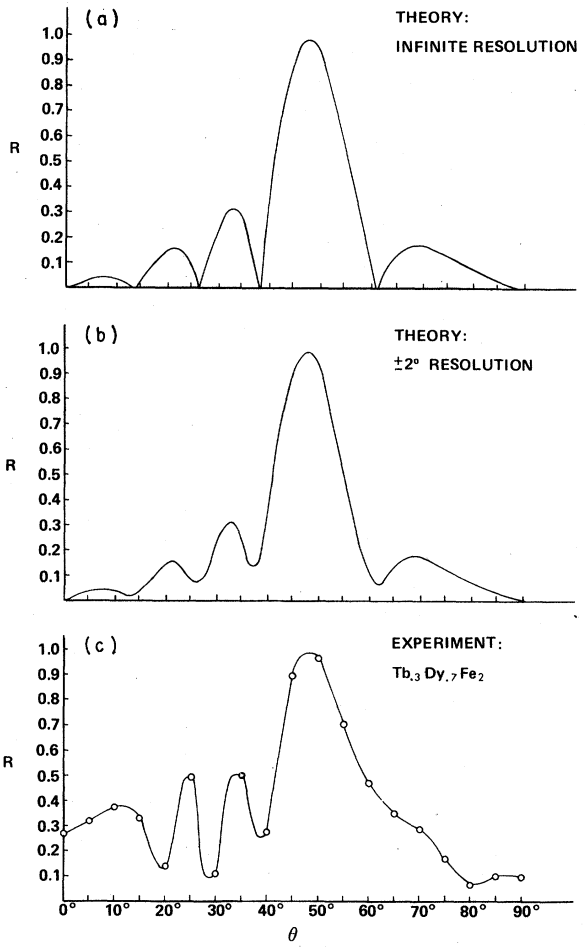

FIG. 5. Comparison of theory and experiment. (a) The amplitude expected at the receiver for the arrangement shown in Fig. 1 and described in the text, based on Eq. (14). (b) The expected amplitude corrected for finite resolution, as described in text. (c) The experimental amplitude at the receiver (points). The line is a guide to the eye.

receiver amplitude as a function of θ for different values of H. The theoretical curve for $H = 8$ kOe is plotted in Fig. 5(a). The envelope, peaked around 45°, is due to sin2Φ while the oscillations come from the interference term. We have also plotted in Fig. 5(b) a modified version of Eq. (14) corrected for depolarization and finite resolution i.e., the curve has been obtained by simply averaging $|R|$ over the resolution interval Δ

$$R'(\theta) = \int_{-\Delta}^{+\Delta} R(\theta + \Phi) d\Phi .$$

The agreement of this prediction with the experimental results shown in Fig. 5(c) for the same value of H (= 8 kOe), is reasonably good; the central peak is reproduced by the theory as well as the characteristics of much of the structure away from the resonance angle. Measurements at values of field from 4 to 10 kOe gave curves with the same general features as the one of Fig. 5(c). At lower fields the amplitude of the signal detected by the receiver was very small and nearly constant. This seems to be related to the lack of magnetic saturation and to the huge attenuation of the C_{44} mode observed in previous pulse-echo measurements of the velocity.[6]

In the range of field in which the resonance could be detected, we measured the orientation θ_R corresponding to the maximum of the central peak [$\theta_R \equiv \theta(\Phi = 45°)$] and we compared it with the theoretical prediction

$$\theta_R = \left\{ \arcsin \left[\frac{M_s H}{b_1^2 + b_2^2} \left(\frac{b_2^2}{M_s H} + \frac{C_{11} - C_{12}}{2} - C_{44} \right) \right] \right\}^{1/2} . \tag{15}$$

θ_R is plotted versus H in Fig. 6, using the values of the parameters listed above. As one can see in Fig. 6, the agreement between theory and experiments is again good, although the limited range of field investigated and the indeterminateness due to the width of the peaks and to the instrumental resolution precludes thorough comparison with the theory. A more convincing check of the linear theory would come from measurements at higher fields, i.e., in the 30–40-kOe range where the theoretical $\theta_R \sim (H_M - H)^{1/2}$. H_M is the maximum field at which resonance can occur.

IV. DISCUSSION

The theory outlined in Sec. II provides a reasonable picture of the resonance and polarization

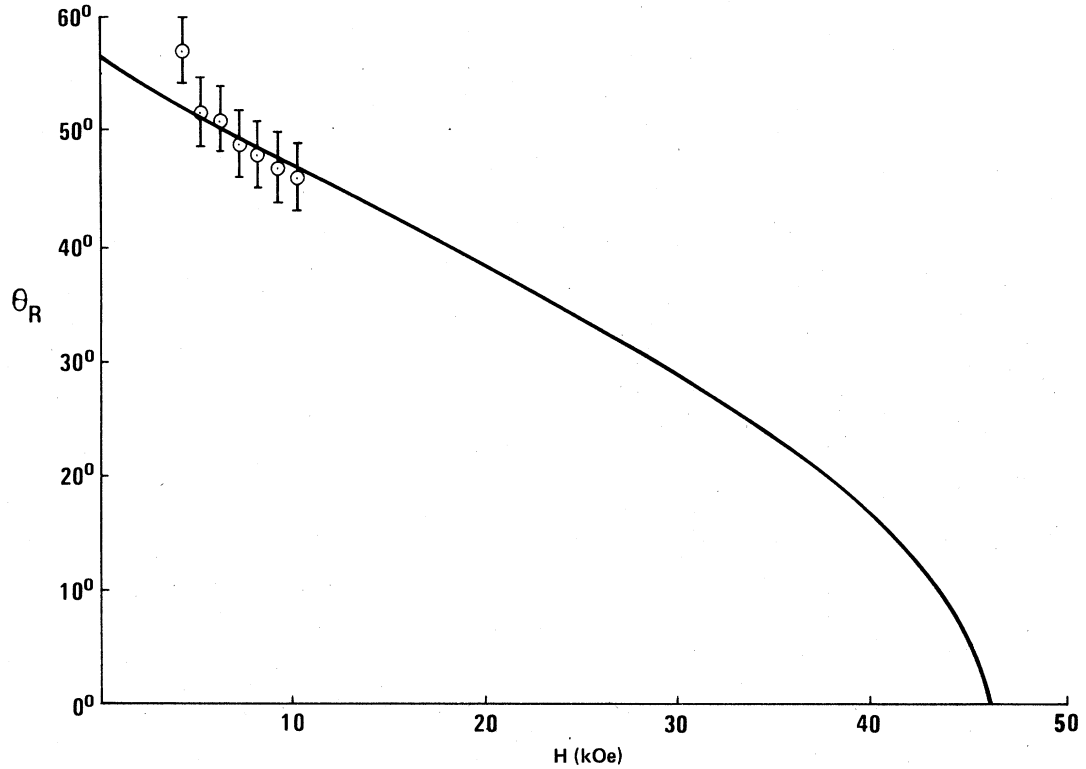

FIG. 6. Angle at which resonance was detected in the amplitude at the receiver plotted versus field. The solid line is the theoretical curve based on Eq. (15) using the parameters given in Table I.

rotations described in Sec. III. Essential to these effects was the requirement that b_1 be nonzero, though small compared to b_2 (to ensure a certain sharpness to the resonance). From the value of b_1 used to compare theory and experiment, i.e., 2×10^8 erg/cm^3 we would expect a relative softening of the $C_{11}-C_{12}$ mode as the magnetic field is rotated in the (110) plane from the [001] to the [$\bar{1}$10] direction, of about 1%. In fact, previous pulse-echo work[6] has shown that the modulus actually stiffens under this rotation by a percent or so. From further study,[10] it was concluded that the variation of the $C_{11}-C_{12}$ modulus with θ is at odds with predictions based on Eq. 1. Clearly there are other magnetoelastic interactions taking place in this alloy whose effects are of the order of or larger than those due to b_1. There are, for example, morphic[11] and higher-order magnetoelastic[4,12] effects which could account for the $C_{11}-C_{12}$ behavior with moment orientation as well as contribute to coupling of $C_{11}-C_{12}$- to C_{44}-type modes in a similar way to the coupling provided by b_1 and b_2. The detailed analysis required to sort out the relevent second-order effects will not be given in this report. Measurements of the resonance angle as a function of field strength (Fig. 6) would provide an experimental way of separating the linear, field-dependent effects from second-order field-independent contributions. Though not a complete description, the linear theory of magnetoelasticity correctly predicts the qualitative features of the receiver amplitude as a function of magnetic field orientation that we observed in the transmission experiment. We feel that the agreement is due to the dominance of the very large b_2 term in the magnetoelastic interaction over the smaller b_1 and second-order terms. In the linear theory, the width of the central peak in the amplitude versus orientation plot (Fig. 5) is determined by b_1. From attempts at making this width equal to the experimental one, we estimate b_1 as 2×10^8 erg/cm^3. In view of the probable presence of second-order magnetoelastic coupling, we regard this as an upper bound to b_1.

We expect it is possible to alter the acoustical polarization in many of the cubic Laves-phase rare-earth–iron compounds. For achieving large changes, it is important to choose pseudobinaries of the form $R^1_xR^2_{1-x}Fe_2$ with x chosen to reduce the magnetic anisotropy. This arrangement can preserve the magnetoelastic coupling and yet allow one to rotate the moment with convenient magnetic field strenghts.

ACKNOWLEDGMENTS

We thank Dr. A. E. Clark for providing the crystal (grown by D. McMasters of Iowa State University) used in the experiment. We also thank Dr. Clark as well as Dr. G. Blessing and Dr. R. Abbundi for helpful discussions during the course of this work.

---

*On leave of absence from MASPEC Laboratory of CNR, Parma, Italy supported in part by Office of Naval Research.

†Supported by Office of Naval Research and NSWC Independent Research Fund.

[1]C. Kittel, *Introduction to Solid State Physics* (Wiley, New York, 1953).

[2]B. Lüthi, Appl. Phys. Lett. 8, 107 (1966).

[3]G. A. Alers, J. R. Neighbours, and H. Sato, J. Phys. Chem. Solids, 9, 21 (1958).

[4]D. E. Eastman, Phys. Rev. 148, 530 (1966).

[5]A. E. Clark, AIP Conf. Proc. 18, 1015 (1974); A. Clark and H. Belson, Phys. Rev. B 5, 3642 (1972).

[6]S. Rinaldi, J. Cullen, and G. Blessing, Phys. Lett. A 61, 465 (1977).

[7]C. Kittel, Phys. Rev. 110, 836 (1958).

[8]G. Simon, Z. Naturforsch A 13, 84 (1958); see also Ref. 3.

[9]R. C. Lecraw & R. L. Comstock, in *Physical Acoustics*, edited by W. P. Mason (Academic, New York, 1956), Vol. III B, p. 127.

[10]J. Cullen, S. Rinaldi, and G. Blessing, J. Appl. Phys. 49, (3) 1960 (1978).

[11]W. P. Mason, Phys. Rev. 82, 715 (1951).

[12]V. Dohm and P. Fulde Z. Phys. B 21, 369 (1975).